First on-line isotopic characterization of N_2O above intensively managed grassland

Running head: Real-time grassland N_2O isotopic signature

[1,2]Benjamin Wolf, [3]Lutz Merbold, [3]Charlotte Decock, [1]Béla Tuzson, [1]Eliza Harris, [3]Johan Six, [1]Lukas Emmenegger, [1]Joachim Mohn

[1]Laboratory for Air Pollution / Environmental Technology, Empa, Überlandstrasse 129, CH-8600 Dübendorf

[2]Institute for Meteorology and Climate Research (IMK-IFU), Karlsruhe Institute or Technology, Kreuzeckbahnstrasse 19, 82467 Garmisch-Partenkirchen

[3]Department of Environmental Systems Science, ETH Zurich, Universitaetsstrasse 2, CH-8092 Zürich

Corresponding author: Benjamin Wolf, benjamin.wolf@kit.edu, +49 8821 183288

Keywords: N_2O, isotopomers, QCLAS, source partitioning, grassland, nitrification, denitrification, N_2O reduction

Paper type: primary research

Abstract

The analysis of the four main isotopic N_2O species ($^{14}N^{14}N^{16}O$, $^{14}N^{15}N^{16}O$, $^{15}N^{14}N^{16}O$, $^{14}N^{14}N^{18}O$) and especially the intramolecular distribution of ^{15}N (site preference, SP) has been suggested as a tool to distinguish source processes and to help constrain the global N_2O budget. However, current studies suffer from limited spatial and temporal resolution capabilities due to the combination of discrete flask sampling with subsequent laboratory-based mass spectrometric analysis. Quantum cascade laser absorption spectroscopy (QCLAS) allows selective high-precision analysis of N_2O isotopic species at trace levels and is suitable for in-situ measurements.

Here, we present results from the first field campaign, conducted on an intensively managed grassland in central Switzerland. N_2O mole fractions and isotopic composition were determined in the atmospheric surface layer (2.2 m height) at high temporal resolution with a modified state-of-the-art laser spectrometer connected to an automated N_2O preconcentration unit. The analytical performance was determined from repeated measurements of a compressed air tank and resulted in measurement repeatability of 0.20, 0.12 and 0.11‰ for $\delta^{15}N^{\alpha}$, $\delta^{15}N^{\beta}$ and $\delta^{18}O$, respectively. Simultaneous eddy-covariance N_2O flux measurements were used to determine the flux-averaged isotopic signature of soil-emitted N_2O.

Our measurements indicate that in general, nitrifier-denitrification and denitrification were the prevalent sources of N_2O during the campaign, and that variations in isotopic composition were rather due to alterations in the extent to which N_2O was reduced to N_2, than other pathways such as hydroxylamine oxidation. Management and rewetting events were characterized by low values of the intra-molecular ^{15}N site preference (SP), $\delta^{15}N^{bulk}$ and $\delta^{18}O$, suggesting nitrifier denitrification and incomplete heterotrophic bacterial denitrification responded most strongly to the induced disturbances. Flux-averaged isotopic composition of N_2O from intensively managed grassland was

43 6.9 ± 4.3, - 17.4 ± 6.2 and 27.4 ± 3.6 ‰ for SP, $\delta^{15}N^{bulk}$ and $\delta^{18}O$, respectively. The approach
44 presented here is capable of providing long-term datasets also for other N_2O emitting ecosystems,
45 which can be used to further constrain global N_2O inventories.
46

1 Introduction

Atmospheric nitrous oxide (N_2O) mole fraction is increasing since pre-industrial times predominately due to increased agricultural activity (Davidson, 2009; Mosier et al., 1998). Owing to the approximately 300 times higher global warming potential (GWP) compared to CO_2, this greenhouse gas (GHG) currently accounts for 6% of total anthropogenic radiative forcing (Myhre et al., 2013). Recent estimates showed that N_2O is in addition the single most important ozone-depleting substance (Ravishankara et al., 2009). Because at least 60% of total anthropogenic N_2O emissions is attributed to food production (Syakila and Kroeze, 2011), growing human population and meat consumption per capita as well as biofuel production will accelerate the rate of increase in atmospheric N_2O concentration. Hence, the development of adequate mitigation strategies is pertinent and requires a better understanding of the processes driving N_2O fluxes. To date, nitrification, nitrifier denitrification and denitrification are considered to constitute the dominant N_2O producing processes, especially in agricultural soils (Wrage et al., 2001). Other N_2O source-processes such as abiotic N_2O production, co-denitrification and heterotrophic nitrification have also been observed; a concise overview of observed processes is given elsewhere (Butterbach-Bahl et al., 2013). This complexity inherent in the N cycle and associated transformation processes is a major challenge in developing mitigation strategies, as attribution of N_2O production to the respective processes is required to tailor target-oriented actions (Baggs, 2008). Approaches for apportioning of N_2O emissions to nitrification, denitrification, and N_2O reduction to N_2 (source partitioning) have mostly relied on acetylene (C_2H_2) inhibition and isotope labeling (Groffman et al., 2006), but denitrification rates are underestimated by the C_2H_2 method (Butterbach-Bahl et al., 2013; Groffman et al., 2006; Watts and Seitzinger, 2000). Isotope labeling approaches are vulnerable to incomplete diffusion of the tracer and to stimulation of process rates by the addition of the labeled substrates themselves (Groffman et al., 2006).

71 Changes in natural abundance of ^{15}N and ^{18}O in N_2O have been explored to investigate N_2O
72 production processes, but the determined $\delta^{15}N$ and $\delta^{18}O$ depend on both fractionation factors and
73 isotopic composition of precursors, which in turn exhibit strong variations (Baggs, 2008; Bedard-
74 Haughn et al., 2003; Heil et al., 2014; Toyoda et al., 2011).
75 N_2O is a linear molecule and four main isotopic species can be discerned: $^{14}N^{14}N^{16}O$, $^{14}N^{15}N^{16}O$,
76 $^{15}N^{14}N^{16}O$ and $^{14}N^{14}N^{18}O$. The isotopic species $^{14}N^{14}N^{16}O$, $^{14}N^{14}N^{18}O$ and $^{14}N^{15}N^{16}O$ (or
77 $^{15}N^{14}N^{16}O$) are isotopologues, while $^{14}N^{15}N^{16}O$ and $^{15}N^{14}N^{16}O$ are isotopomers and will be
78 termed $^{15}N^{\alpha}$-N_2O and $^{15}N^{\beta}$-N_2O (Toyoda and Yoshida, 1999). The umbrella term isotopocule is
79 used for both isotopomers and isotopologues. The intra-molecular distribution of ^{15}N in N_2O
80 ('site preference'; $SP = \delta^{15}N^{\alpha} - \delta^{15}N^{\beta}$) has been reported to be independent of the substrate's
81 isotopic composition, as SP in the de novo produced N_2O remained constant even though $\delta^{15}N$
82 and $\delta^{18}O$ values of both N_2O and substrates changed markedly during experiments with pure
83 cultures (Heil et al., 2014; Sutka et al., 2003, 2006, 2008; Toyoda et al., 2005). Therefore, SP can
84 be considered as a tracer conserving the source process information (Ostrom and Ostrom, 2011).
85 The SP of different processes has been characterized in a number of pure-culture, mixed culture
86 (Ostrom et al., 2007; Sutka et al., 2003, 2006; Toyoda et al., 2005; Wunderlin et al., 2012, 2013),
87 and soil-incubation studies (Köster et al., 2011, 2013a; Lewicka-Szczebak et al., 2014; Well et
88 al., 2006, 2008) with a compilation of data in Toyoda et al. (2011). A recent review on source
89 partitioning and SP (Decock and Six, 2013b) concluded that SP is capable of distinguishing
90 between the process groups N_2O_N (NH_2OH-oxidation, fungal denitrification and abiotic N_2O
91 production; $SP = 32.8 \pm 4.0$ ‰) and N_2O_D (nitrifier-denitrification and denitrification; $SP = -$
92 1.6 ± 3.8 ‰). In addition, N_2O isotopocules can be used as an independent validation of the
93 global, measurement-based bottom-up N_2O budget and has already confirmed that the

isotopically light sources such as agriculture and industry contribute to the increase in atmospheric N_2O (Toyoda et al., 2013; Yoshida and Toyoda, 2000). Owing to the temporal and spatial variability of isotopomer ratios, it is indispensable to derive flux-weighted average values from different sources (such as ecosystems) for later use in budget analysis using box models (Kim and Craig, 1993; Perez et al., 2001; Yoshida and Toyoda, 2000).

N_2O isotopomers can be measured by mass spectrometry, but it requires discrete flask sampling with subsequent laboratory analysis. Hence, this approach is limited in temporal resolution and spatial representation of a given site. Additionally it is indirect, as information on the site-specific isotopic composition is derived from the analysis of the NO^+ fragment and N_2O^+ molecular ion. Recently, a quantum cascade laser absorption spectrometer (QCLAS) capable of selective analysis of the three most abundant N_2O isotopocules has been presented (Waechter et al., 2008) and its potential for in-situ measurements in conjunction with an automated pre-concentration unit has been shown (Mohn et al., 2010, 2012). Here we present the results obtained from a, to our knowledge worldwide first, campaign in which the isotopic composition of N_2O (SP, $\delta^{15}N$, $\delta^{18}O$) in the atmospheric surface layer was determined on-line by using an optimized state-of-the-art laser spectrometer. With the combination of N_2O isotopic analysis by QCLAS, accompanying eddy-covariance based N_2O flux measurements as well as monitoring of environmental conditions and inorganic nitrogen concentrations, our specific objectives for this study were: i) to demonstrate the capability of QCLAS systems for high precision isotopic analysis of (soil emitted) N_2O in ambient air; ii) to investigate management and weather effects on isotopic composition and source processes; and iii) to characterize the flux-averaged isotopic composition of N_2O emitted from an intensively managed grassland.

2 Material and Methods

2.1 Study site

The agricultural research station Chamau (CHA) is located in Central Switzerland at an elevation of 400 m a.s.l.. The experiment was conducted on an intensively managed grassland belonging to CHA which is primarily used for fodder production and occasional winter grazing by sheep (Zeeman et al., 2010). The soil type is a cambisol with a bulk density of 0.97g cm^{-3}, 30.6 % sand, 47.7 % silt and 21.8 % clay in the top 10 cm and pH of 5.7-6.2. Soil carbon and nitrogen content in the top 10 cm was 37.9 g kg^{-1} and 4.1 g kg^{-1} (Roth, 2006). Mean annual temperature and annual precipitation are 9.1°C and 1151 mm, respectively (Zeeman et al., 2010). Management practices aim at fodder production and consist of mowing followed by slurry application, with up to six mowing/slurry applications per year and occasional grazing of sheep and cattle in October and November. During the campaign in summer 2013, three management cycles were carried out. Harvest dates were June 6th, July 11th and August 21st and slurry was applied within 10 days after each mowing event. Nitrogen input was calculated from the applied amount of slurry brought to the field and the N concentration determined (Labor für Boden- und Umweltanalytik, Eric Schweizer AG, Thun, Switzerland) in a sample drawn from the supply to the trailing hose applicator. The applied N amounted to 30, 40 and 43.3 kg N ha^{-1} for the first, second and third application, respectively. The grassland is re-established via ploughing and resowing approximately every 10 years. The last re-establishment event took place in 2012 (Merbold et al., 2014).

2.2 Instrumental setup for analysis of N_2O isotopocule ratios

The four most abundant N_2O isotopic species were quantified using a modified QCLAS (Aerodyne Research Inc., Billerica MA, USA) equipped with a continuous wave quantum cascade laser (cw-QCL) with spectral emission at 2203 cm^{-1}, an astigmatic Herriott multi-pass

absorption cell (204 m path length, AMAC-200), and reference path with a short (5 cm) N_2O–filled cell to lock the laser emission frequency (Tuzson et al., 2013). During the campaign, the QCLAS was operated in an air-conditioned trailer located 60 m west of the eddy-covariance (EC) tower. This trailer position contributes < 20 % to the main flux and is at the far side of prevailing wind direction (Zeeman et al., 2010). The sample air inlet was installed next to the inlet of the EC tower (2.2 m height). Sample air was drawn through a PTFE tube (4 mm ID) by a membrane pump (PM 25032-022, KNF Neuberger, Switzerland). Upstream of the pump, the sample air was pre-dried with a permeation drier (MD-050-72S-1, PermaPure Inc., USA). Following the pump, the pressure was maintained at 4 bar overpressure using a pressure relieve valve. Humidity, as well as CO_2, were quantitatively removed from the gas flow by applying a chemical trap filled with Ascarite (7 g, 10 – 35 mesh, Fluka, Switzerland) bracketed by $Mg(ClO_4)_2$ (2 x 1.5 g, Fluka, Switzerland). Finally, the sample gas was passed through a sintered metal filter (SS-6F-MM-2, Swagelok, USA) and directed to a preconcentration unit described in detail previously (Mohn et al., 2010, 2012). For an increase of N_2O mixing ratios from ambient level to around 50 ppm N_2O, approx. 8 litres of ambient air were preconcentrated. Afterwards, the preconcentrated N_2O was introduced into the evacuated multi-pass cell of the QCLAS. Isotopic fractionation during preconcentration (increase by 0.31 ± 0.10, 0.34 ± 0.16 and 0.29 ± 0.07 ‰ for $\delta^{15}N^{\alpha}$, $\delta^{15}N^{\beta}$ and $\delta^{18}O$, respectively) was quantified by preconcentration of N_2O with a known isotopic composition and subsequently corrected. Compatibility of N_2O isotopomer analysis by QCLAS with isotope ratio mass spectrometry (IRMS) laboratories was recently demonstrated in an inter-laboratory comparison campaign (Mohn et al., 2014).

2.3 Measurement and calibration strategy

To ensure high accuracy and repeatability of the analytical system, a measurement and calibration strategy similar to the one presented by Mohn et al. (2012) was applied. It is based on

two standard gases differing in N_2O isotopic composition, which were produced by dynamic dilution of pure medical N_2O (Pangas, Switzerland) with defined amounts of isotopically pure (>98 %) $^{14}N^{15}N^{16}O$ (Cambridge Isotope Laboratories, USA) and (>99.95 %) $^{14}N^{14}NO$ (ICON Services Inc., USA). Subsequent gravimetric dilution with high purity synthetic air (99.999 %, Messer Schweiz AG) resulted in pressurized gas mixtures with 90 ppm N_2O (parts per million, 10^{-6} moles of trace gas per mole of dry air). Both standards were calibrated against primary standards which were previously measured by the Tokyo Institute of Technology (TIT, Toyoda and Yoshida) to anchor δ-values to the international isotopic standard scales. The first standard (S1, Table 1) was used as an anchor point to international δ-scale and used as input data for data analysis algorithms (see data processing). Therefore, the N_2O isotopic composition of S1 was targeted to closely resemble background air. As the N_2O isotopic composition of surface layer air is mainly a mixture of soil-derived and background composition, the second standard (S2, Table 1) used for span correction was depleted in $\delta^{15}N^{\alpha}$, $\delta^{15}N^{\beta}$ and $\delta^{18}O$ compared to background air in accordance with the expected terrestrial source signatures.

The measurement protocol started with the injection of S1, dynamically diluted to 50 ppm, the mole fraction of ambient N_2O after preconcentration. After flushing the absorption cell with synthetic air, S2 was injected, also diluted to 50 ppm. For determination of the slight concentration dependence already reported (Mohn et al., 2012), S1 was injected again but at a higher mole fraction of 67 ppm (later referred to as $S1_h$). This mole fraction represents the mole fraction expected after preconcentration of high concentration surface layer air. Subsequently, S1 was injected again, diluted to 50 ppm, before the cell was filled with preconcentrated ambient N_2O (A). This subroutine (S1+A) of injection of S1 and preconcentrated ambient N_2O took 35 minutes and was repeated three times. For an independent determination of repeatability, the

fourth sample was preconcentrated compressed air (target gas). During the campaign, two compressed air cylinders (C1 and C2, referred to as target gas) were used. Isotopic composition and N_2O mixing ratio of both cylinders were determined in the laboratory prior to campaign start (Table 1). N_2O mole fractions and isotopic composition analysed in the laboratory and at the field site agreed within their analytical uncertainty. Following target gas analysis, S1 and $S1_h$ were analyzed again. Another set of three subroutines S1+A completed one run. One complete cycle of 6 ambient air samples and one compressed air sample took 340 minutes, leading to approx. 25 ambient air samples being analysed during 24 hours. N_2O mole fractions were determined according to Mohn et al. (2012).

2.4 Data processing

Data processing is based on individual mixing ratios of the four main N_2O isotopic species and spectrometer characteristics as recorded by the instruments's software (TDLWintel, Aerodyne Research Inc., Billerica, MA, USA). In the first step, variations in the isotope ratios induced by drifts in the instrument working parameters during the field operation were corrected. A linear additive model explaining the deviation of isotope ratios R^{α}, R^{β} and R^{18O} for repeated measurements of standard S1 from their mean value by absorption cell temperature (T1), laser temperature (T2), line position (LP) and pressure (p) was calibrated based on S1 injections. For isotope ratios of S1, $S1_h$, S2, sample air and compressed air, these systematic deviations were corrected based on the respective values of T1, T2, LP and p. In a second step, concentration dependence of isotope ratios, determined using the measurements of S1 and $S1_h$, was addressed with corrections (0.013, 0.028 and 0.004 ‰ ppb^{-1} for $\delta^{15}N^{\alpha}$, $\delta^{15}N^{\beta}$ and $\delta^{18}O$) being in the same range as described earlier (Mohn et al., 2012). Subsequently, remaining drifts were corrected based on analysis of S1. Finally, isotope ratios were converted to δ-values using a 2-point calibration derived from corrected values of S1 and S2.

2.5 Determination of soil-emitted N_2O isotopic composition

Isotopic composition of the source process "soil N_2O emission" was derived using the Keeling plot approach (Keeling, 1958), where δ-values measured (here in 2.2 m height) are plotted versus the inverse of N_2O mole fractions. The intercept of the linear regression line can be interpreted as the isotopic composition of soil emitted N_2O (Pataki et al., 2003). Therefore, determination of soil N_2O isotopic composition requires an increase in N_2O mole fraction. During the day, turbulence mixes surface layer air to the atmospheric background. At night, the surface layer becomes more stable and the N_2O mole fraction increases, shifting isotopic composition towards its source composition. As a consequence, Keeling plots were based on noon-to-noon periods. This approach is discussed in section 4.6.

2.6 N_2O Flux measurement

At CHA, greenhouse gas mole fractions, including N_2O, are measured continuously since 2012 by means of the eddy covariance (EC) method (Baldocchi and Meyers, 1998). The system consists of a three-dimensional sonic anemometer to measure wind speed and direction (2.41 m height, Solent R3, Gill Instruments, Lymington, UK) and a QCLAS (mini-QCLAS, Aerodyne Research Inc., Billerica, MA, USA) to determine N_2O mole fractions at a temporal resolution of 10 Hz. Both data streams are merged near-real time within a data acquisition system (MOXA embedded Linux computer; Moxa, Brea, CA, USA) via an RS-232 serial data link (Eugster and Plüss, 2010). The setup has been described in detail previously (Merbold et al., 2014). Post-processing of N_2O fluxes included screening for obvious out-of-range values (+/- 100 nmol $m^{-2}s^{-1}$). N_2O fluxes were further aggregated to noon-to-noon daily averages to smoothen the large variability in the 30 min flux averages. Daily averages were calculated for days where more than 30 half-hour values were available, with this filter excluding three days from analysis.

2.7 Soil inorganic N, dissolved organic C and environmental conditions

Ammonium (NH_4^+) and nitrate (NO_3^-) concentrations were determined from soil (0-20 cm depth) sampled at 10 positions along a transect within the footprint of the EC measurements following the predominant wind direction. Samples were taken weekly throughout the campaign or daily during mowing and slurry application events. Per sample, ~15 g of fresh soil were added to specimen vessels containing 50 ml 1M KCl. After 1 hour on a shaker, the supernatant was filtered (Whatman no.42 ashless filter paper, 150 mm diameter) and analysed colorimetrically for NH_4^+ and NO_3^-. For a subset of extracts, we determined dissolved organic carbon (DOC) concentrations by combustion of KCl extracts using a total organic C analyzer (Shimdazu TOC-V, Columbia, MD, USA).

Soil temperatures and volumetric soil moisture contents at 10 cm depth were measured at the same 10 locations along the transect (5TM-sensors, Decagon Devices Ltd., Pullman, USA). Data were stored as 10 minute averages on a data logger (EM50, Decagon Devices Ltd., Pullman, USA). The volumetric water content was converted to water filled pore space (wfps) using a bulk density of 1.09 g cm^{-3}. Precipitation was measured with a tipping bucket rain gauge (Type 10116, Toss GmbH, Potsdam, Germany) and stored as 10 min averages on a data logger (CR10X-2M, Campbell Scientific Inc., Logan, USA).

3 Results

3.1 Long term precision for target gas analysis

System performance for N_2O mole fractions and isotopic composition was determined based on repeated analysis of compressed air from target gas tanks (C1, C2). There was no significant drift in the δ-values and N_2O mole fractions, indicating stability of the applied measurement technique. Repeatability, calculated as the standard deviation (σ) of 331 target gas measurements, amounted to 0.20, 0.12, 0.10, 0.12 and 0.22 ‰ for $\delta^{15}N^{\alpha}$, $\delta^{15}N^{\beta}$, $\delta^{18}O$, $\delta^{15}N^{bulk}$ and SP, respectively (Figure 1). Standard deviation for the N_2O mole fraction of the target gas was 0.25 ppb.

3.2 N_2O mole fractions and isotopic composition at 2.2 m height

Air samples were taken at 2.2 m height which is within the lowest 10% of the atmospheric boundary layer (ABL) where mechanical generation of turbulence exceeds buoyant generation or consumption. This part of the ABL is called surface layer, hence corresponding air samples are referred to as surface layer air samples. N_2O isotopic composition of the surface layer air samples (n = 2130) ranged from 2.5 to 16.1 ‰, -11.9 to -2.4 ‰, 37.6 to 44.6 ‰, -4.6 to 6.6 ‰, and 14.3 to 19.3 ‰ for $\delta^{15}N^{\alpha}$, $\delta^{15}N^{\beta}$, $\delta^{18}O$, $\delta^{15}N^{bulk}$ and SP, respectively (Figure 2). Surface layer N_2O mole fractions varied between 325 and 469 ppb and followed a diurnal cycle with highest values during the night when the boundary layer became more stable. Increasing N_2O mole fractions were associated with decreasing δ-values, indicating that soil emitted N_2O that mixed into the surface layer was depleted in ^{15}N as compared to N_2O in the atmospheric background.

3.3 Auxiliary measurements

Half hourly N_2O fluxes were averaged from noon-to-noon (f_{N2O}), and ranged from -1 to 5 nmol m^{-2} s^{-1}. Maximum N_2O fluxes coincided with an overnight build up in N_2O mole fractions (ΔN_2O) as analysed by QCLAS and could not be attributed to slurry application events alone (Figure 3). Among the correlations of f_{N2O} and auxiliary variables, only the one with nitrate concentration ($r^2 = 0.18$) was significant ($p<0.01$). Soil water content (wfps) was modulated by precipitation and two clear states could be identified. During the "wet" part of the campaign lasting until July 7th, average wfps was with 62 ± 4 % significantly (t-test, $p < 0.001$) higher than the average of 37 ± 4 % calculated for the remainder of the campaign (referred to as the "dry" part). Soil temperature did not show such a clear two-phase pattern, however temperatures during the first, "wet" part were with 16.7±4 °C significantly ($p<0.001$) lower than during the "dry" phase with 21.2±2 °C.

Background NH_4^+ and NO_3^- concentrations were smaller than 3 μg g_{soil}^{-1} and clearly responded to mowing and slurry application in the second and third management events. The NO_3^- concentration was higher than the NH_4^+ concentration and peaked at 16 and 50 μg g_{soil}^{-1}, while NH_4^+ concentration peaked at 9 and 15 μg g_{soil}^{-1} for these two management events. In contrast, dissolved organic carbon concentrations (DOC) did not respond to management events, but were higher during the "dry" phase of the campaign ($p < 0.001$).

3.4 Isotopic composition of soil-emitted N_2O

The uncertainty of the determined source isotopic composition was estimated based on the standard error of the Keeling plot intercept and depends on the degree to which soil air accumulated in the surface layer (ΔN_2O, Figure 4). For instance, the intercept (source) standard error ranged from 0.3 to 82 ‰ for SP. To apply the Keeling plot approach only to situations in

296 which soil air accumulated in the surface layer, only source isotopic compositions for overnight
297 increases in N_2O mole fractions of more than 12 ppb were considered in this study. This filter
298 lead to a maximum and average (μ) standard error of 6.8 (μ=2.2) ‰, 4.5 (μ=1.4) ‰ and 2.2
299 (μ=1) ‰ for SP, $\delta^{15}N^{bulk}$ and $\delta^{18}O$ isotopic source signatures, respectively.

300 During the field campaign, Keeling plot derived isotopic composition of soil-emitted N_2O ranged
301 from 1.4 to 17.3 ‰, -29 to -3 ‰ and 22.6 to 34.8 ‰ for SP, $\delta^{15}N^{bulk}$ and $\delta^{18}O$, respectively. All
302 explanatory variables except NH_4^+ and NO_3^- were found to significantly correlate with SP (Table
303 2). For $\delta^{15}N^{bulk}$, correlations with ΔN_2O, wfps, soil temperature, DOC and $NO_3^-$and for $\delta^{18}O$
304 correlations of f_{N2O}, ΔN_2O, precipitation, soil temperature and NO_3^-were significant. However,
305 the adjusted r^2 for all regressions was below 0.4; in addition, multiple explanatory variables such
306 as NH_4^+ and NO_3^- or wfps and temperature (Figure 5) did not increase the explained variance
307 above this value.

308 ## 3.5 Event-based data aggregation

309 As already described in the section "Auxiliary measurements", there was a "wet" phase (n=27
310 Keeling-plot derived N_2O isotopic compositions) in the beginning of the campaign, which lasted
311 about one month and a "dry" phase lasting about two months (n=38). Therefore, the dataset was
312 split in two corresponding parts with averages of 7.4 ± 3.6 ‰ versus 11.1 ± 4.2 ‰ for SP, -
313 19 ± 3.8 ‰ versus -12.5 ± 5.9 ‰ for $\delta^{15}N^{bulk}$ and 28.7 ± 2.2 ‰ versus 29.7 ± 3.4 ‰ for $\delta^{18}O$ in
314 the wet versus the dry phase, respectively. Averages of SP and $\delta^{15}N^{bulk}$ were significantly
315 different ($p < 0.001$) but $\delta^{18}O$ averages were not. Based on this simple classification, the dry
316 phase contains rewetting events. A rewetting event was defined as a two day period starting at the
317 day for which wfps increased. Exclusion of these rewetting events during the dry phase increased
318 average δ-values (n=30) as well as decreased standard deviations for SP, $\delta^{15}N^{bulk}$ and $\delta^{18}O$ to

319 12.5 ± 3.4, -10.8 ± 4.5 and 30.7 ± 2.8 ‰. Moreover the difference in $\delta^{18}O$ was significant ($p <$
320 0.001).

321 In addition to the dry/wet classification, we also defined three subsets representing the N_2O
322 emission associated with management events of mowing followed by fertilization ("Mana I" –
323 "Mana III"), one subset representing a rewetting event between Mana II and III ("Rewetting")
324 and one subset representing background ("BG", all remaining measurements). There were two
325 distinct rewetting events between management events II and III, but N_2O isotopic composition is
326 only available for the first one (07/29/2014 - 07/31/2014). Isotopic compositions of soil-emitted
327 N_2O were assigned to subsets of management or rewetting if the associated flux or nutrient
328 concentration was elevated. This classification scheme led to 3 to 7 measurements for
329 management and rewetting events (Figure 3, underlaid in transparent blue) while 47 measurements
330 were assigned to class BG. Boxplots for SP, $\delta^{15}N^{bulk}$, $\delta^{18}O$, and wfps (Figure 6) showed
331 characteristic δ-values and wfps for management and rewetting, but not for subset BG.
332 Measurements assigned to BG covered practically the whole range of values observed across all
333 the other classes. Therefore, standard deviations for class BG were one order of magnitude larger
334 than for the four other classes.

335 Statistical analysis is confounded by low and unequal sample size so that we compared
336 exclusively the subsets management and rewetting using multiple non-parametric Wilcoxon tests
337 after having checked homogeneity of variances using Bartlett test. For all investigated δ-values,
338 only differences between groups Mana II and Mana III were significant.

339 ### 3.6 Averages of N_2O isotopic signature for intensively managed grassland

340 Simple averages of daily isotopic composition of soil-emitted N_2O were 9.6 ± 4.4, -15.2 ± 6.0
341 and 29.3 ± 3 ‰ for SP, $\delta^{15}N^{bulk}$ and $\delta^{18}O$, respectively (n=62). Representative isotopic

composition of N_2O emitted from a given site or treatment can be estimated based on flux-weighted averages of daily isotopic composition. For some noon-to-noon periods included in the above average, thus with an overnight increase in N_2O mole fractions of at least 12 ppb, negative N_2O fluxes were detected by the EC system (-0.17 ± 2.1 nmol $m^{-2}s^{-1}$; n=14). This might be due to the uncertainty of N_2O flux measurements, temporal averaging over positive and negative fluxes in a noon-to-noon period or different footprint regions for N_2O flux and isotopic analysis (flux vs. concentration footprint). To avoid bias to the flux-weighted average of emitted N_2O by either one of the above mentioned possible reasons, the weighted averages were calculated for positive flux events only. Flux weighted averages were 6.9 ± 4.3, - 17.4 ± 6.2 and 27.4 ± 3.6 ‰ for SP, $\delta^{15}N^{bulk}$ and $\delta^{18}O$ respectively (n=48).

4 Discussion

4.1 Analytical performance

To our knowledge, only two pilot studies exist demonstrating the potential of QCLAS based analytical techniques for on-line and high-precision analysis of N_2O mole fractions and isotopic composition in surface layer air. While Mohn et al. (2012) analyzed the three most abundant ^{15}N-isotopocules ($^{14}N^{14}N^{16}O$, $^{15}N^{14}N^{16}$, $^{14}N^{15}N^{16}O$), Harris et al. (2014a) included the ^{18}O isotopologue ($^{14}N^{14}N^{18}O$). In both studies, however, the instrument was located in the laboratory. Based on three weeks of measurements, Mohn et al. (2012) reported a precision of 0.24 and 0.17 ‰ for $\delta^{15}N^{\alpha}$ and $\delta^{15}N^{\beta}$, respectively and Harris et al. (2014a) reported 0.17, 0.19 and 0.32 ‰ for $\delta^{15}N^{\alpha}$, $\delta^{15}N^{\beta}$ and $\delta^{18}O$, respectively, for a twelve days period. In both studies, analytical performance was determined, in accordance with the presented study, based on repeated analysis of compressed air samples. Thereby, the analytical precision reached in the presented study, was distinctly higher for $\delta^{15}N^{\beta}$ and $\delta^{18}O$ and similar for $\delta^{15}N^{\alpha}$ compared to these two previous studies, even though the measurements were done under field-conditions and over a much longer, three months, period. This confirms the high level of precision associated with QCLAS based determination of N_2O isotopic composition. Standard errors for Keeling plot intercepts (Figure 4) confirm that this precision is sufficient to resolve the variability of atmospheric N_2O sampled close to the ground. As our instrument was located directly at the field site and measurements were conducted over a period of more than three months, our study indicates that this level of repeatability can be achieved both at long time scales and in the field.

4.2 N_2O isotopic composition in the atmospheric surface layer (2.2 m height)

In our study, δ-values of single preconcentrated air samples were between atmospheric background and 14.3 ‰ (SP) and -4.7 ‰ ($\delta^{15}N^{bulk}$). Mohn et al. (2012) reported similar values between atmospheric background and 12 ‰ (SP) and -4 ‰ ($\delta^{15}N^{bulk}$). Therefore the variation

observed in both studies is much higher compared to the measurements by Harris et al. (2014a) where the N_2O isotopic composition deviated only slightly from atmospheric background. A consistent decrease in $\delta^{15}N^{bulk}$ in parallel with increasing N_2O mole fractions (accumulation of soil-derived N_2O) confirms that the soil N_2O source is depleted in ^{15}N-N_2O relative to ambient N_2O (Toyoda et al., 2013). A similar pattern was found for $\delta^{18}O$; an increase in N_2O mole fraction was associated with a decrease in ^{18}O-N_2O, again indicating that soil emissions were depleted in ^{18}O-N_2O with respect to the atmospheric background. In contrast, Harris et al. (2014a) reported a decoupling of $\delta^{18}O$ and $\delta^{15}N^{bulk}$. This may have been due to only marginal influence of soil-emitted N_2O since the measurements were carried out in urban area and approx. 95 m above the ground. Studies on N_2O derived from combustion processes indicate that some of these sources might be less depleted or even enriched in ^{15}N-N_2O compared to ambient N_2O (Harris et al., 2014b; Ogawa and Yoshida, 2005).

4.3 Isotopic composition of soil-emitted N_2O

SP of soil-emitted N_2O observed in our study (1 to 17 ‰) is within the ranges expected for a mixture of the two process groups N_2O_N and N_2O_D, and does not necessarily indicate significant contribution of N_2O reduction, an effect which is discussed further below. Isotopic composition of soil-emitted N_2O has been predominately determined in laboratory incubation studies (Köster et al., 2013a, 2013b; Perez et al., 2006; Well and Flessa, 2009b; Well et al., 2006, 2008). Additionally, results from field experiments using static chambers (Opdyke et al., 2009; Ostrom et al., 2010; Toyoda et al., 2011; Yamulki et al., 2001) and N_2O accumulation below a snowpack have been published (Mohn et al., 2013). Based on pure culture studies SP values from 19.7 to 40 ‰ and -8.7 to 8.5 ‰, were observed for N_2O_N and N_2O_D, respectively (Decock and Six, 2013b). In field experiments SP was found to range between -1 and 32 ‰ (Opdyke et al., 2009), -3 and 18 ‰ (Yamulki et al., 2001), -14 and 90 ‰ (Toyoda et al., 2011) and 0 and 13 ‰ (Ostrom

et al., 2010). The very high SP values detected by Toyoda et al. (2011) may have resulted from extensive N_2O reduction to N_2, a process increasing SP, $\delta^{15}N^{bulk}$ and $\delta^{18}O$ (Ostrom et al., 2007). For $\delta^{15}N^{bulk}$ and $\delta^{18}O$, a much wider variation as compared to SP is expected, because these variables depend both on fractionation factors, which vary among different microbial communities and depend on reaction conditions, as well as on the isotopic composition of the substrate (Baggs, 2008). Under field conditions, $\delta^{15}N^{bulk}$ was reported to range between -17 and 9 ‰ (Opdyke et al., 2009), -27 and 1 ‰ (Yamulki et al., 2001), -44 and 34 ‰ (Toyoda et al., 2011) and -18 and -15 ‰ (Ostrom et al., 2010), covering the range of -29 to -3 ‰ observed in this study. With respect to $\delta^{18}O$, the values of 22.6 to 34.8 ‰ detected for grassland in this study are at the lower end of measurements under field conditions (4-82 ‰).

4.4 Changes in N_2O source signatures induced by N_2O reduction to N_2

Quantitative source partitioning between process groups N_2O_N and N_2O_D based on SP is possible only when no other processes except those contained in the process groups have an influence on the site-specific N_2O isotopic composition. However, in the terminal step of denitrification, namely the reduction of N_2O to N_2, N-O bonds between lighter isotopes are cleaved preferentially, leading to an increase in SP, $\delta^{15}N^{bulk}$ and $\delta^{18}O$ in the remaining N_2O. Consequently, part of the N_2O originating from a combination of the two process groups, i.e. N_2O_N and N_2O_D, may have been consumed by N_2O to N_2 reduction prior to emission.

For identification of processes determining N_2O isotopic composition, isotopocule maps were suggested in which site preference is plotted versus the difference in substrate and product isotopic composition (Koba et al., 2009). Determination of isotopic composition in the substrates is time consuming and additionally confounded in our study by the large and varying footprint area. Therefore, we present a modified isotope map of SP versus $\delta^{15}N^{bulk}$ (Figure 7, left panel)

instead of $\Delta\delta^{15}N$, the $\delta^{15}N$ differences between substrate and product (i.e. N_2O gas). Rectangles for process groups N_2O_N and N_2O_D are defined by SP values given by Decock and Six (2013b) and by $\delta^{15}N^{bulk}$ values calculated based on process fractionation factors and substrate isotopic composition. For nitrification and denitrification minimum and maximum fractionation factors of -90 to -40 ‰ and -40 to -15 ‰ were assumed (Baggs, 2008), for the isotopic compositions of the N_2O precursors (i.e., NH_4^+ and NO_3^-) a range of -20 to +10 ‰ and -25 to 15 ‰ were assumed. Koba et al. (2009) attributed a concurrent decrease in $\delta^{15}N^{bulk}$ with increasing SP values as indicative for an increasing contribution of N_2O_N. In contrast, an increase in $\delta^{15}N^{bulk}$ in parallel to increasing SP values (enrichment of ^{15}N in the α-position relative to the β-position), as observed in the present study, was allocated to a substantial increase in N_2O reduction to N_2. Our results (Figure 7, left panel) indicate that N_2O is predominately formed by bacterial denitrification, and that deviations in the isotope values from denitrification may have been caused by variations in the extent to which N_2O was reduced to N_2. It is noteworthy that based on such modified isotope maps, systematic changes in $\delta^{15}N^{bulk}$ induced by systematic changes in N isotopic composition of one of the precursors NH_4^+ or NO_3^- could be misinterpreted as reduction events (Well et al., 2012).

In addition to the SP/$\delta^{15}N^{bulk}$ maps, SP/$\delta^{18}O$ maps have been suggested to trace N_2O reduction to N_2 (Lewicka-Szczebak et al., 2014, 2015; Well et al., 2012). While $\delta^{15}N^{bulk}$ depends on the isotopic composition of the precursor (e.g. NO_3^-) and, thus, may vary considerably, $\delta^{18}O$-N_2O is expected to be more stable as during both nitrification and denitrification, oxygen (O) later found in N_2O may almost completely originate from water (Kool et al., 2009). Due to this almost complete O-exchange with water, relatively stable $\delta^{18}O$ in soil water, and the observed constant ratio of fractionation factors for SP and $\delta^{18}O$-N_2O ($r_{sp\text{-}o}$), variation in the share of N_2O reduced to

N_2 should be reflected by a linear relationship between SP and $\delta^{18}O$-N_2O with a slope of 0.2-0.5 (Jinuntuya-Nortman et al., 2008; Ostrom et al., 2007; Well and Flessa, 2009a). In this study, a linear relationship with a slope of 1.02 was found (Figure 7, right panel). Tracking the management events (ManaI to ManaIII) and the rewetting event in SP/$\delta^{18}O$ space revealed that the onset of such an event is associated with a decrease of both SP and $\delta^{18}O$, gradually increasing back to approximately initial values, except for ManaII. During ManaII, no significant change in SP/$\delta^{18}O$ occurred (Figure 7, right panel, red trace). The gradual increase in isotopic composition supports the conclusion from the SP/$\delta^{15}N^{bulk}$ map that N_2O was mainly produced by bacterial denitrification and that variations in isotopic composition may have been caused predominately by N_2O reduction to N_2. This interpretation is in agreement with observations of isotopoic composition of N_2O, NO_3^- and NH_4^+ during a rewetting event in an agricultural field (Decock and Six, 2013a). Additionally, $\delta^{18}O$ was found to be positively correlated with $\delta^{15}N^{bulk}$, which enforces the interpretation that varying shares of N_2O reduction occurred because it acts on both N and O isotopic composition (Koehler et al., 2012).

As introduced above, the ratios of fractionation factors for $\delta^{18}O$ and $\delta^{15}N^{bulk}$ ($r_{o\text{-}n}$) and SP and $\delta^{18}O$ ($r_{sp\text{-}o}$) during N_2O reduction were 2.5 and 0.2 to 0.5 in laboratory incubation experiments (Jinuntuya-Nortman et al., 2008; Ostrom et al., 2007; Well and Flessa, 2009a). In our study, $r_{o\text{-}n}$ and $r_{sp\text{-}o}$ were 0.5 and 1, respectively for the whole dataset. We calculated these ratios also for a subset of data for which all δ-values (SP, $\delta^{15}N^{bulk}$ and $\delta^{18}O$) increased for two consecutive days, indicating that N_2O reduction may have occurred. Such events were observed on 8 occasions. If source processes (N_2O_D, N_2O_N) contributed constantly over two consecutive measuring days, changes in the isotopic composition of emitted N_2O were solely attributed to changes in the fraction of N_2O reduction. Under such conditions one would expect that the ratio of the changes

in $\delta^{18}O$ and $\delta^{15}N^{bulk}$ ($r_{o\text{-}n}$) is around 2.5 and that the ratio of the changes in SP and $\delta^{18}O$ ($r_{sp\text{-}o}$) is between 0.2 and 0.5. The mean (median) ratios for $r_{o\text{-}n}$ and $r_{sp\text{-}o}$ for these selected events were 0.69 (0.44) and 2.1 (1.16), respectively. While the high values of $r_{sp\text{-}o}$ indicate that for instance changing physical conditions such as soil moisture may play a role in field measurements, the deviation of $r_{o\text{-}n}$ from the value of 2.5 could either indicate that the fractionation factor for ^{18}O might be smaller than the one for ^{15}N or that there is no correlation of fractionation factors in natural environments. This is in line with recent findings showing that apparent isotope effects associated with N_2O reduction are sensitive to experimental conditions which influenced diffusive isotope effects (Lewicka-Szczebak et al., 2014, 2015). The same study also showed that fractionation factors during N_2O reduction for ^{15}N and ^{18}O were variable (from -11 to +12 ‰ and from -18 to +4 ‰, respectively), and not predictable for field conditions yet. Therefore, to date, the amount of N_2O reduction prior to emission cannot be inferred with sufficient robustness from field measurements alone, without the knowledge of isotopic composition of the substrates.

4.5 Controls on isotopic composition and event based data aggregation

The high temporal resolution of N_2O isotopic and auxiliary measurements allowed us to investigate controls on N_2O isotopic composition over the 3 months campaign period. Correlations with isotopic composition were highest and positive for DOC and soil temperature (Table 2). The significant correlation with temperature for the whole campaign was due to a significant correlation during the "dry" part of the campaign. If the increase in SP was due to increased contribution of nitrification, $\delta^{15}N^{bulk}$ should decrease due to the higher isotopic fractionation during this process. The simultaneous increase in SP, $\delta^{15}N^{bulk}$ and $\delta^{18}O$ revealed in Figure 7, however, indicates an increased share of N_2O reduction to N_2 which might have been triggered by increased substrate availability (DOC) for heterotrophic denitrification. The reported effect of temperature on the N_2O:N_2 ratio is not without any doubt, but a decrease has been

observed with increasing temperature, supporting the hypothesis that N_2O reduction increased as temperature rose throughout the measurement period (Saggar et al., 2013).

Though substrate availability has been identified as a major control on N_2O source processes (see references in Saggar et al., 2013), correlations between N_2O isotopic composition and NO_3^- and NH_4^+ concentrations were low, except for the correlation with $\delta^{15}N^{bulk}$. The reason might be both the number of measurment points for substrate concentrations being lower compared to other explanatory variables and substrate concentrations not necessarily reflecting process or turnover rates (Wu et al., 2012).

The low explanatory power of all linear regressions underlines that drivers for N_2O emissions are highly variable and may even change from event to event. In absence of management or rewetting events (group BG), isotopic composition covered the whole range of measured values, while management or rewetting events were characterized by lower variability in isotopic composition. Values for SP, $\delta^{15}N^{bulk}$ and $\delta^{18}O$ were low for Mana I, rewetting and Mana III, whereas event Mana II showed increased SP, $\delta^{15}N^{bulk}$ and $\delta^{18}O$. This indicates that processes must have been different for Mana II, although management was almost identical.

4.6 Short term variation of isotopic composition

The Keeling plot approach is based on conservation of mass and assumes that the atmospheric concentration of a gas in the surface layer is a mixture of background atmospheric concentration and a variable amount of gas added by a source, raising the atmospheric concentration above background. The source's isotope value can be determined given that its isotope value remains constant during the observation period. In this study, we used noon-to-noon data in the Keeling plots to determine isotope values of soil-derived N_2O for the respective noon-to-noon period. Hence, the source processes underlying these N_2O emissions have to be constant on this time

517 scale. Currently, little is known about the rate of change of N_2O source processes over time-steps
518 of minutes to hours. However, changing relative contributions of source processes, which change
519 the isotopic composition in soil-emitted N_2O, would be reflected by deviations from a linear
520 relation between inverse concentration and isotopic composition. As the Keeling plots showed no
521 obvious deviations from a linear relation within our measurement precision (See supplementary
522 file S1), we conclude (1) that the use of the Keeling plot approach was valid in our study, and (2)
523 that changes in N_2O source processes in our study site occurred at a time step of one day or more.
524 While our data suggests that there are little or no changes in source processes underlying N_2O
525 emissions within a noon-to-noon period, clear and distinct day-to-day variation in isotope values
526 of soil derived N_2O, especially in SP, were observed. Such changes were often strong and abrupt
527 following management events (ManaI & III, Rewetting), indicating a significant response of
528 microbial processes to the imposed disturbance. Larger than expected variability in isotope values
529 was observed in-between management events (class BG), when no obvious variation in
530 environmental drivers occurred. Since noon-to-noon concentration increases were very small
531 during these periods, part of this variability may be attributed to increased uncertainty around the
532 intercept of the Keeling plot. This is also reflected in the relatively large error bars around isotope
533 values on days when overnight N_2O concentration increase was low (Figure 3). Alternatively, the
534 variation in isotope values associated with small overnight concentration increase may result
535 from other land use or land cover. The EC fluxes are calculated from the turbulent fluctuation of
536 concentration and vertical wind speed (i.e. the covariance of the concentration and wind speed
537 deviations from the half-hourly mean) and therefore account for the modulation of concentration
538 around a short term (30 min) mean caused by locally emitted N_2O. Isotopic composition based on
539 Keeling plots however is determined from total N_2O accumulated in the nocturnal boundary layer
540 and, thus, this approach also contains molecules that had been emitted outside the flux footprint,

which almost exclusively comprised our grassland site (Zeeman et al., 2010), within the larger concentration footprint (Griffis et al., 2007). However, two facts indicate a major influence of the studied grassland on the determined N_2O isotopic composition: First, the N_2O isotopic composition is very stable for a noon-to-noon period as indicated by a linear relationship between individual measurements (supplementary file S1). This relationship persists even though wind speed and direction are changing and, therefore, individual N_2O isotope mesurements integrating over 16 minutes sampling interval originate from different source areas. Secondly, the CHA grassland can be characterized as a site with vigorous N_2O emission and therefore may dominate the determined N_2O isotopic composition as the influence of a source area increment scales with the source strength. The grassland was restored in 2012 which lead to extraordinary high N_2O-N emission of 29.1 kg ha^{-1} $year^{-1}$ (Merbold et al., 2014). In the following year 2.5 kg N_2O-N ha^{-1} were released. This value is still in the range of maximum emissions reported for another intensively managed Swiss grassland, emitting 1.5-2.6 kg N ha^{-1} $year^{-1}$ and at least a factor of five compared to an extensively managed grassland with less than 0.5 kg N ha^{-1} $year^{-1}$ (Ammann et al., 2009). With regard to distant land use and land cover, the 2.5 kg N_2O-N are also more than double the median (between the 70 and 75 percentile) of all reported values for cultivated temperate sites and higher than the highest value reported for forests presented in a study containing 1008 N_2O emission measurements from agricultural fields (Stehfest and Bouwman, 2006). However, it cannot be excluded that N_2O isotopic signatures analyzed above the grassland were influenced by adjacent ecosystems.

4.7 Flux weighted averages of source isotopic compositions

N_2O isotopic composition can be used to calculate and further constrain the global N_2O budget (Kim and Craig, 1993; Yoshida and Toyoda, 2000). The analysis of emissions from different sources such as agricultural soils or managed grasslands based on box models and isotopic

composition is complicated by distinct temporal and spatial variability of isotopic composition (Kim and Craig, 1993; Toyoda et al., 2011; Yoshida and Toyoda, 2000); hence, flux weighted averages are required to obtain representative values for agricultural N_2O (Perez et al., 2001). Our flux weighted averages of 6.9 ± 4.3, -17.4 ± 6.2 and 27.4 ± 3.6 ‰ for SP, $\delta^{15}N^{bulk}$ and $\delta^{18}O$ are well within the range of values 2.9 to 36.6, -41.5 to -1.9 and 23.2 to 51.7 ‰ for agricultural soils (Park et al., 2011; Toyoda et al., 2011). The comparison with other grassland soils (Opdyke et al., 2009; Park et al., 2011) indicates that the variability of isotopic composition within a group, such as grassland, may be considerable (for SP: 2.2 to 11.1 ‰). One has to keep in mind, however, that part of the observed variability may be attributed to the fact that the footprint area of the N_2O isotopic composition includes areas with other land use or land cover. Another part of the variability might be also explained by a limited compatibility of laboratory results, as recently demonstrated in an inter-laboratory comparison campaign (Mohn et al., 2014). The uncertainty in budgets derived by isotopic composition depends on the uncertainty of the representative isotopic composition for a single source, which can be reduced by a quasi-continuous measurement approach, as shown in this study.

5 Conclusion

Our field observations indicate that nitrifier-denitrification and denitrification (process group N_2O_D) dominated throughout the measurement period and that variation in isotopic composition was more likely due to variation in the extent of N_2O reduction rather than contributions of NH_2OH oxidation or fungal denitrification. High temporal resolution of isotopic composition in soil-emitted N_2O showed that at the beginning of the growing season, medium wfps and low temperature induced low isotope values (representative for process group N_2O_D), whereas in the second part of the measurement period, higher temperature and DOC stimulated N_2O reduction to

588 N_2, although wfps was lower. Management or rewetting events were mostly characterized by low
589 SP, $\delta^{15}N^{bulk}$ and $\delta^{18}O$, but the event Mana II indicated that processes underlying N_2O emissions
590 can vary even under similar management conditions. With this study, a new method is available
591 that can provide real-time datasets for various single N_2O emitting (eco)systems, such as as
592 grasslands or agricultural soils, which will help in further constraining the global N_2O budget
593 based on box model calculations. However, future campaigns should be accompanied by
594 footprint modeling for optimization of the inlet height and associated concentration footprint size.
595

Acknowledgements

We are grateful to Hans-Ruedi Wettstein and his team for the collaboration with the ETH research station Chamau and Christoph Zellweger for support with determination of GHG mixing ratios in our target gases. Antoine Roth is acknowledged for his support during the field campaign. This project was funded by the State Secretariat for Education and Research (SER) within COST Action ES0806. The QCLAS used for EC measureents was funded by the R'Equip Project (206021 133763) by the Swiss National Science Foundation. Funding form GHG-Europe (FP7, EU contract No. 244122) and COST Action ES0804 - ABBA is gratefully acknowledged. Instrumental developments at Empa were supported by the Swiss National Science Foundation (SNSF). Technical support on the eddy covariance station has been provided by Thomas Baur and Peter Plüss. Preparation of N_2O isotope standards and inter-laboratory comparison measurements were supported by the EMRP ENV52 project 'Metrology for high-impact greenhouse gases'. The EMRP is jointly funded by the EMRP participating countries within EURAMET and the European Union.

612

613 **References**

614 Ammann, C., Spirig, C., Leifeld, J. and Neftel, A.: Assessment of the nitrogen and carbon budget
615 of two managed temperate grassland fields, Agric. Ecosyst. Environ., 133(3-4), 150–162,
616 doi:10.1016/j.agee.2009.05.006, 2009.

617 Baggs, E. M.: A review of stable isotope techniques for N_2O source partitioning in soils : recent
618 progress , remaining challenges and future considerations, Rapid Commun. Mass Spectrom., 22,
619 1664–1672, doi:10.1002/rcm, 2008.

620 Baldocchi, D. and Meyers, T.: On using eco-physiological, micrometeorological and
621 biogeochemical theory to evaluate carbon dioxide, water vapor and trace gas fluxes over
622 vegetation: a perspective, Agric. For. Meteorol., 90(1-2), 1–25, doi:10.1016/S0168-
623 1923(97)00072-5, 1998.

624 Bedard-Haughn, A., van Groenigen, J. W. and van Kessel, C.: Tracing ^{15}N through landscapes:
625 potential uses and precautions, J. Hydrol., 272(1-4), 175–190, doi:10.1016/S0022-
626 1694(02)00263-9, 2003.

627 Butterbach-Bahl, K., Baggs, E. M., Dannenmann, M., Kiese, R. and Zechmeister-Boltenstern, S.:
628 Nitrous oxide emissions from soils : how well do we understand the processes and their controls?,
629 Philos. Trans. R. Soc. B-Biological Sci., 368, 20130122, 2013.

630 Davidson, E. A.: The contribution of manure and fertilizer nitrogen to atmospheric nitrous oxide
631 since 1860, Nat. Geosci., 2(9), 659–662, 2009.

632 Decock, C. and Six, J.: An assessment of N-cycling and sources of N_2O during a simulated rain
633 event using natural abundance ^{15}N, Agric. , Ecosyst. Environ., 165, 141–150, 2013a.

634 Decock, C. and Six, J.: How reliable is the intramolecular distribution of ^{15}N in N_2O to source
635 partition N_2O emitted from soil?, Soil Biol. Biochem., 65(2), 114–127,
636 doi:10.1016/j.soilbio.2013.05.012, 2013b.

637 Eugster, W. and Plüss, P.: A fault-tolerant eddy covariance system for measuring CH_4 fluxes,
638 Agric. For. Meteorol., 150(6), 841–851, doi:10.1016/j.agrformet.2009.12.008, 2010.

639 Griffis, T. J., Zhang, J., Baker, J. M., Kljun, N. and Billmark, K.: Determining carbon isotope
640 signatures from micrometeorological measurements: Implications for studying biosphere–
641 atmosphere exchange processes, Boundary-Layer Meteorol., 123(2), 295–316,
642 doi:10.1007/s10546-006-9143-8, 2007.

643 Groffman, P. M., Altabet, M. A., Bohlke, J. K., Butterbach-Bahl, K., David, M. B., Firestone, M.
644 K., Giblin, A. E., Kana, T. M., Nielsen, L. P. and Voytek, M. A.: Methods for measuring
645 denitrification: Diverse approaches to a difficult problem, Ecol. Appl., 16(6), 2091–2122, 2006.

646 Harris, E., Nelson, D. D., Olszewski, W., Zahniser, M., Potter, K. E., McManus, B. J., Whitehill,
647 A., Prinn, R. G. and Ono, S.: Development of a Spectroscopic Technique for Continuous Online
648 Monitoring of Oxygen and Site-Specific Nitrogen Isotopic Composition of Atmospheric Nitrous
649 Oxide., Anal. Chem., doi:10.1021/ac403606u, 2014a.

650 Harris, E., Zeyer, K., Kegel, R., Müller, B., Emmenegger, L. and Mohn, J.: Nitrous oxide
651 emissions and isotopic composition from waste incineration in Switzerland, Waste Manag.,
652 submitted, 2014b.

653 Heil, J., Wolf, B., Brüggemann, N., Emmenegger, L., Tuzson, B., Vereecken, H. and Mohn, J.:
654 Site-specific ^{15}N isotopic signatures of abiotically produced N_2O, Geochim. Cosmochim. Acta,
655 139, 72–82, doi:10.1016/j.gca.2014.04.037, 2014.

656 Jinuntuya-Nortman, M., Sutka, R. L., Ostrom, P. H., Gandhi, H. and Ostrom, N. E.: Isotopologue
657 fractionation during microbial reduction of N_2O within soil mesocosms as a function of water-
658 filled pore space, Soil Biol. Biochem., 40(9), 2273–2280, doi:10.1016/j.soilbio.2008.05.016,
659 2008.

660 Keeling, C. D.: The concentration and isotopic abundances of atmospheric carbon dioxide in
661 rural areas, Geochim. Cosmochim. Acta, 13, 322–334, doi:10.1016/0016-7037(58)90033-4,
662 1958.

663 Kim, K. R. and Craig, H.: Nitrogen-15 and oxygen-18 characteristics of nitrous oxide: a global
664 perspective., Science, 262(5141), 1855–7, doi:10.1126/science.262.5141.1855, 1993.

665 Koba, K., Osaka, K., Tobari, Y., Toyoda, S., Ohte, N., Katsuyama, M., Suzuki, N., Itoh, M.,
666 Yamagishi, H., Kawasaki, M., Kim, S. J., Yoshida, N. and Nakajima, T.: Biogeochemistry of
667 nitrous oxide in groundwater in a forested ecosystem elucidated by nitrous oxide isotopomer
668 measurements, Geochim. Cosmochim. Acta, 73(11), 3115–3133, doi:10.1016/j.gca.2009.03.022,
669 2009.

670 Koehler, B., Corre, M. D., Steger, K., Well, R., Zehe, E., Sueta, J. P. and Veldkamp, E.: An in-
671 depth look into a tropical lowland forest soil: nitrogen-addition effects on the contents of N_2O,
672 CO_2 and CH_4 and N_2O isotopic signatures down to 2-m depth, Biogeochemistry, 111(1-3), 695–
673 713, doi:10.1007/s10533-012-9711-6, 2012.

674 Kool, D. M., Wrage, N., Oenema, O., Harris, D. and Groenigen, J. W. Van: The ^{18}O signature of
675 biogenic nitrous oxide is determined by O exchange with water, Rapid Commun. Mass
676 Spectrom., 23, 104–108, doi:10.1002/rcm, 2009.

677 Köster, J. R., Cárdenas, L., Senbayram, M., Bol, R., Well, R., Butler, M., Mühling, K. H. and
678 Dittert, K.: Rapid shift from denitrification to nitrification in soil after biogas residue application

as indicated by nitrous oxide isotopomers, Soil Biol. Biochem., 43(8), 1671–1677, doi:10.1016/j.soilbio.2011.04.004, 2011.

Köster, J. R., Well, R., Dittert, K., Giesemann, A., Lewicka-Szczebak, D., Mühling, K.-H., Herrmann, A., Lammel, J. and Senbayram, M.: Soil denitrification potential and its influence on N_2O reduction and N_2O isotopomer ratios., Rapid Commun. mass Spectrom., 27(21), 2363–73, doi:10.1002/rcm.6699, 2013a.

Köster, J. R., Well, R., Tuzson, B., Bol, R., Dittert, K., Giesemann, A., Emmenegger, L., Manninen, A., Cárdenas, L. and Mohn, J.: Novel laser spectroscopic technique for continuous analysis of N_2O isotopomers--application and intercomparison with isotope ratio mass spectrometry., Rapid Commun. Mass Spectrom., 27(1), 216–22, doi:10.1002/rcm.6434, 2013b.

Lewicka-Szczebak, D., Well, R., Bol, R., Gregory, A. S., Matthews, G. P., Misselbrook, T., Whalley, W. R. and Cardenas, L. M.: Isotope fractionation factors controlling isotopocule signatures of soil-emitted N_2O produced by denitrification processes of various rates, Rapid Commun. Mass Spectrom., 29, 269–282, doi:10.1002/rcm.7102, 2015.

Lewicka-Szczebak, D., Well, R., Köster, J. R., Fuß, R., Senbayram, M., Dittert, K. and Flessa, H.: Experimental determinations of isotopic fractionation factors associated with N_2O production and reduction during denitrification in soils, Geochim. Cosmochim. Acta, 134, 55–73, doi:10.1016/j.gca.2014.03.010, 2014.

Merbold, L., Eugster, W., Stieger, J., Zahniser, M., Nelson, D. and Buchmann, N.: Greenhouse gas budget (CO_2 , CH_4 and N_2O) of intensively managed grassland following restoration., Glob. Chang. Biol., 20(6), 1913–1928, doi:10.1111/gcb.12518, 2014.

Mohn, J., Guggenheim, C., Tuzson, B., Vollmer, M. K., Toyoda, S., Yoshida, N. and Emmenegger, L.: A liquid nitrogen-free preconcentration unit for measurements of ambient N_2O isotopomers by QCLAS, Atmos. Meas. Tech., 3(3), 609–618, doi:10.5194/amt-3-609-2010, 2010.

Mohn, J., Steinlin, C., Merbold, L., Emmenegger, L. and Hagedorn, F.: N_2O emissions and source processes in snow-covered soils in the Swiss Alps., Isotopes Environ. Health Stud., 49(4), 520–31, doi:10.1080/10256016.2013.826212, 2013.

Mohn, J., Tuzson, B., Manninen, A., Yoshida, N., Toyoda, S., Brand, W. A. and Emmenegger, L.: Site selective real-time measurements of atmospheric N_2O isotopomers by laser spectroscopy, Atmos. Meas. Tech., 5(7), 1601–1609, doi:10.5194/amt-5-1601-2012, 2012.

Mohn, J., Wolf, B., Toyoda, S., Lin, C. T., Liang, C. M., Brüggemann, N., Wissel, H., Steiker, A. E., Dyckmans, J., Szwek, L., Ostrom, N. E., Casciotti, K. L., Forbes, M., Giesemann, A., Well, R., Doucett, R. R., Yarnes, C. T., Ridley, A. R., Kaiser, J. and Yoshida, N.: Inter-Laboratory assessment of notrous oxide isotopomer analysis of isotopomer analysis by isotope ratio mass spectrometry and laser spectroscopy: current status and perspectives, Rapid Commun. Mass Spectrom., 28, 1995–2007, 2014.

Mosier, A., Kroeze, C., Nevison, C., Oenema, O., Seitzinger, S. and van Cleemput, O.: Closing the global N_2O budget: nitrous oxide emissions through the agricultural nitrogen cycle - OECD/IPCC/IEA phase II development of IPCC guidelines for national greenhouse gas inventory methodology, Nutr. Cycl. Agroecosystems, 52(2-3), 225–248, 1998.

Myhre, G., Shindell, D., Bréon, F.-M., Collins, W., Fuglestvedt, J., Huang, J., Koch, D., Lamarque, L., Mendoza, B., Nakaijima, T., Robock, A., Stephens, G., Takemura, T. and Zhang, H.: Anthropogenic and Natural Radiative Forcing, in Climate Change 2013: The Physical Science Basis. Contribution of Working Group I to the Fifth Assessment Report of the Intergovernmental Panel on Climate Change, edited by T. Stocker, D. Qin, P. GK, M. Tignor, S. Allen, J. Boschung, A. Nauels, Y. Xia, V. Bex, and P. Midgley, pp. 659–740, Cambridge University Press, Cambridge, UK and New York, NY, USA., 2013.

Ogawa, M. and Yoshida, N.: Intramolecular distribution of stable nitrogen and oxygen isotopes of nitrous oxide emitted during coal combustion., Chemosphere, 61(6), 877–87, doi:10.1016/j.chemosphere.2005.04.096, 2005.

Opdyke, M. R., Ostrom, N. E. and Ostrom, P. H.: Evidence for the predominance of denitrification as a source of N_2O in temperate agricultural soils based on isotopologue measurements, Global Biogeochem. Cycles, 23(4), GB4018 1–10, doi:10.1029/2009GB003523, 2009.

Ostrom, N. E. and Ostrom, P. H.: The Isotopomers of Nitrous Oxide: Analytical Considerations and Application to Resolution of Microbial Production Pathways, in Handbook of Envirionmental Isotope Geochemistry Volume 1, edited by M. Baskaran, pp. 453–476, Springer Berlin Heidelberg, Berlin, Heidelberg., 2011.

Ostrom, N. E., Pitt, A., Sutka, R. L., Ostrom, P. H., Grandy, A. S., Huizinga, K. M. and Robertson, G. P.: Isotopologue effects during N_2O reduction in soils and in pure cultures of denitrifiers, J. Geophys. Res., 112(G2), 1–12, doi:10.1029/2006JG000287, 2007.

Ostrom, N. E., Sutka, R. L., Ostrom, P. H., Grandy, A. S., Huizinga, K. M., Gandhi, H., von Fischer, J. C. and Robertson, G. P.: Isotopologue data reveal bacterial denitrification as the primary source of N_2O during a high flux event following cultivation of a native temperate grassland, Soil Biol. Biochem., 42(3), 499–506, doi:10.1016/j.soilbio.2009.12.003, 2010.

Park, S., Pérez, T., Boering, K. A., Trumbore, S. E., Gil, J., Marquina, S. and Tyler, S. C.: Can N_2O stable isotopes and isotopomers be useful tools to characterize sources and microbial pathways of N_2O production and consumption in tropical soils?, Global Biogeochem. Cycles, 25(1), 1–16, doi:10.1029/2009GB003615, 2011.

Pataki, D., Ehleringer, J., Flanagan, L., Yakir, D., Bowling, D., Still, C., Buchmann, N., Kaplan, J. and Berry, J.: The application and interpretation of Keeling plots in terrestrial carbon cycle research, Global Biogeochem. Cycles, 17(1), doi:10.1029/2001GB001850, 2003.

Perez, T., Garcia-Montiel, D. C., Trumbore, S. E., Tyler, S., de Camargo, P. B., Moreira, M., Piccolo, M. C. and Cerri, C.: Nitrous Oxide Nitrification and Denitrification ^{15}N Enrichment Factros from Amazon Forest Soils, Ecol. Appl., 16(6), 2153–2167, 2006.

Perez, T., Trumbore, S. E., Tyler, S. C., Matson, P. A., Ortiz-Monasterio, I., Rahn, T. and Griffith, D. W. T.: Identifying the agricultural imprint on the global N_2O budget using stable isotopes, J. Geophys. Res., 106(D9), 9869–9878, 2001.

Ravishankara, A. R., Daniel, J. S. and Portmann, R. W.: Nitrous oxide (N_2O): the dominant ozone-depleting substance emitted in the 21st century., Science (80)., 326(5949), 123–5, doi:10.1126/science.1176985, 2009.

Roth, K.: Bodenkartierung und GIS-basierte Kohlenstoffinventur von Graslandböden, 132 pp., University of Zürich (UZH)., 2006.

Saggar, S., Jha, N., Deslippe, J., Bolan, N. S., Luo, J., Giltrap, D. L., Kim, D.-G., Zaman, M. and Tillman, R. W.: Denitrification and N_2O:N_2 production in temperate grasslands: processes, measurements, modelling and mitigating negative impacts., Sci. Total Environ., 465, 173–95, doi:10.1016/j.scitotenv.2012.11.050, 2013.

Stehfest, E. and Bouwman, L.: N_2O and NO emission from agricultural fields and soils under natural vegetation: summarizing available measurement data and modeling of global annual emissions, Nutr. Cycl. Agroecosystems, 74(3), 207–228, 2006.

Sutka, R. L., Adams, G. C., Ostrom, N. E. and Ostrom, P. H.: Isotopologue fractionation during N_2O production by fungal denitrification, Rapid Commun. Mass Spectrom., 22, 3989–3996, doi:10.1002/rcm, 2008.

Sutka, R. L., Ostrom, N. E., Ostrom, P. H., Breznak, J. A., Pitt, A. J., Li, F. and Gandhi, H.: Distinguishing Nitrous Oxide Production from Nitrification and Denitrification on the Basis of Isotopomer Abundances, Appl. Environ. Microbiol., 72(1), 638–644, doi:10.1128/AEM.72.1.638, 2006.

Sutka, R. L., Ostrom, N. E., Ostrom, P. H., Gandhi, H. and Breznak, J. A: Nitrogen isotopomer site preference of N_2O produced by Nitrosomonas europaea and Methylococcus capsulatus Bath., Rapid Commun. Mass Spectrom., 17(7), 738–45, doi:10.1002/rcm.968, 2003.

Syakila, A. and Kroeze, C.: The global nitrous oxide budget revisited, Greenh. Gas Meas. Manag., 1(1), 17–26, doi:10.3763/ghgmm.2010.0007, 2011.

Toyoda, S., Kuroki, N., Yoshida, N., Ishijima, K., Tohjima, Y. and Machida, T.: Decadal time series of tropospheric abundance of N_2O isotopomers and isotopologues in the Northern Hemisphere obtained by the long-term observation at Hateruma Island, Japan, J. Geophys. Res. Atmos., 118(8), 3369–3381, doi:10.1002/jgrd.50221, 2013.

786 Toyoda, S., Mutobe, H., Yamagishi, H., Yoshida, N. and Tanji, Y.: Fractionation of N_2O
787 isotopomers during production by denitrifier, Soil Biol. Biochem., 37(8), 1535–1545,
788 doi:10.1016/j.soilbio.2005.01.009, 2005.

789 Toyoda, S., Yano, M., Nishimura, S., Akiyama, H., Hayakawa, A., Koba, K., Sudo, S., Yagi, K.,
790 Makabe, A., Tobari, Y., Ogawa, N. O., Ohkouchi, N., Yamada, K. and Yoshida, N.:
791 Characterization and production and consumption processes of N_2O emitted from temperate
792 agricultural soils determined via isotopomer ratio analysis, Global Biogeochem. Cycles, 25(2), 1–
793 17, doi:10.1029/2009GB003769, 2011.

794 Toyoda, S. and Yoshida, N.: Determination of Nitrogen Isotopomers of Nitrous Oxide on a
795 Modified Isotope Ratio Mass Spectrometer, Anal. Chem., 71(20), 4711–4718, 1999.

796 Tuzson, B., Zeyer, K., Steinbacher, M., McManus, J. B., Nelson, D. D., Zahniser, M. S. and
797 Emmenegger, L.: Selective measurements of NO, NO_2 and NO_y in the free troposphere using
798 quantum cascade laser spectroscopy, Atmos. Meas. Tech., 6(4), 927–936, doi:10.5194/amt-6-
799 927-2013, 2013.

800 Waechter, H., Mohn, J., Tuzson, B., Emmenegger, L. and Sigrist, M. W.: Determination of N_2O
801 isotopomers with quantum cascade laser based absorption spectroscopy., Opt. Express, 16(12),
802 9239–44, 2008.

803 Watts, S. H. and Seitzinger, S. P.: Denitrification rates in organic and mineral soils from riparian
804 sites : a comparison of N_2 flux and acetylene inhibition methods, Soil Biol. Biochem., 32, 1383–
805 1392, 2000.

806 Well, R., Eschenbach, W., Flessa, H., von der Heide, C. and Weymann, D.: Are dual isotope and
807 isotopomer ratios of N_2O useful indicators for N_2O turnover during denitrification in nitrate-
808 contaminated aquifers?, Geochim. Cosmochim. Acta, 90, 265–282,
809 doi:10.1016/j.gca.2012.04.045, 2012.

810 Well, R. and Flessa, H.: Isotopologue enrichment factors of N_2O reduction in soils, Rapid
811 Commun. Mass Spectrom., 23, 2996–3002, doi:10.1002/rcm, 2009a.

812 Well, R. and Flessa, H.: Isotopologue signatures of N2O produced by denitrification in soils, J.
813 Geophys. Res., 114(G2), 1–11, doi:10.1029/2008JG000804, 2009b.

814 Well, R., Flessa, H., Xing, L., Xiaotang, J. and Römheld, V.: Isotopologue ratios of N_2O emitted
815 from microcosms with NH_4^+ fertilized arable soils under conditions favoring nitrification, Soil
816 Biol. Biochem., 40(9), 2416–2426, doi:10.1016/j.soilbio.2008.06.003, 2008.

817 Well, R., Kurganova, I., Lopesdegerenyu, V. and Flessa, H.: Isotopomer signatures of soil-
818 emitted N_2O under different moisture conditions—A microcosm study with arable loess soil, Soil
819 Biol. Biochem., 38(9), 2923–2933, doi:10.1016/j.soilbio.2006.05.003, 2006.

820 Wrage, N., Velthof, G. L., van Beusichem, M. L. and Oenema, O.: Role of nitrifier denitrification
821 in the production of nitrous oxide, Soil Biol. Biochem., 33(12-13), 1723–1732, 2001.

Wu, H., Dannenmann, M. D., Wolf, B., Han, X. G., Zheng, X. and Butterbach-Bahl, K.: Seasonality of soil microbial nitrogen turnover in continental steppe soils of Inner Mongolia, Ecosphere, 3(4), 34, 2012.

Wunderlin, P., Lehmann, M. F., Siegrist, H., Tuzson, B., Joss, A., Emmenegger, L. and Mohn, J.: Isotope signatures of N_2O in a mixed microbial population system: constraints on N_2O producing pathways in wastewater treatment., Environ. Sci. Technol., 47(3), 1339–48, doi:10.1021/es303174x, 2013.

Wunderlin, P., Mohn, J., Joss, A., Emmenegger, L. and Siegrist, H.: Mechanisms of N_2O production in biological wastewater treatment under nitrifying and denitrifying conditions., Water Res., 46(4), 1027–37, doi:10.1016/j.watres.2011.11.080, 2012.

Yamulki, S., Toyoda, S., Yoshida, N., Veldkamp, E., Grant, B. and Bol, R.: Diurnal fluxes and the isotopomer ratios of N_2O in a temperate grassland following urine amendment., Rapid Commun. Mass Spectrom., 15(15), 1263–9, doi:10.1002/rcm.352, 2001.

Yoshida, N. and Toyoda, S.: Constraining the atmospheric N_2O budget from intramolecular site preference in N_2O isotopomers, Nature, 405(6784), 330–4, doi:10.1038/35012558, 2000.

Zeeman, M., Hiller, R., Gilgen, A. K., Michna, P., Plüss, P., Buchmann, N. and Eugster, W.: Management and climate impacts on net CO_2 fluxes and carbon budgets of three grasslands along an elevational gradient in Switzerland, Agric. For. Meteorol., 150(4), 519–530, doi:10.1016/j.agrformet.2010.01.011, 2010.

Tables

Table 1: Reference gas and compressed air tanks used during the campaign. S1 and S2 represent the anchor and calibration standard. C1 and C2 are the target gases used for determination of system performance. The reported precision is the 1σ standard deviation.

Tank	$\delta^{15}N^{\alpha}$ [‰]	$\delta^{15}N^{\beta}$ [‰]	$\delta^{18}O$ [‰]	$\delta^{15}N^{bulk}$ [‰]	SP [‰]	mixing ratio [ppm] / [ppb]*
S1	15.66 ± 0.03	-3.22 ± 0.13	34.89 ± 0.05	6.22 ± 0.07	18.88 ± 0.13	90.09 ± 0.01
S2	10.38 ± 0.03	-10.55 ± 0.1	25.44 ± 0.06	-0.09 ± 0.05	20.93 ± 0.10	87.28 ± 0.003
C1	15.40 ± 0.08	-3.04 ± 0.06	43.65 ± 0.08	6.18 ± 0.05	18.44 ± 0.10	327.01 ± 0.05
C2	15.65 ± 0.17	-4.27 ± 0.08	44.20 ± 0.07	5.69 ± 0.09	19.92 ± 0.19	327.45 ± 0.05

* ppm for S1 and S2, ppb for C1, C2

852 **Table 2: Adjusted r^2 and p-values for regression analysis of Keeling-plot derived isotopic compositions in soil-emitted N_2O**
853 **versus auxiliary variables N_2O flux (f_{N2O}), difference of maximum and minimum concentration over a noon-to-noon**
854 **period (ΔN_2O), precipitation (prcp), soil moisture (wfps) and nutrient concentrations (NO_3^-, NH_4^+ and DOC).**

855

explanatory	SP r^2	SP p	$\delta^{15}N^{bulk}$ r^2	$\delta^{15}N^{bulk}$ p	$\delta^{18}O$ r^2	$\delta^{18}O$ p	N
f_{N2O}	0.14	**	0.04	0.06	0.16	**	62
ΔN_2O	0.09	*	0.1	*	0.11	*	65
prcp	0.24	**	0.03	0.08	0.24	**	62
wfps	0.14	*	0.29	**	-0.009	0.52	65
T	0.22	**	0.30	**	0.12	*	65
DOC	0.23	*	0.30	*	0.03	0,23	18
NO_3^-	0.04	0.14	0.27	*	0.16	*	31
NH_4^+	-0.03	0.75	-0.03	0.89	-0.03	0.93	31
Significance codes: *: p < 0.05; **: p < 0.001. sample size (n) differs due to data availabilities.							

856

857

Figure legends

Figure 1: Long-term stability (standard deviation σ) derived by target gas injections (n=331) over a 3-month period. As two target gas tanks were used, histograms show deviation of respective tank means, $\bar{x}$, for $\delta^{15}N^{\alpha}$, $\delta^{15}N^{\beta}$, $\delta^{18}O$, $\delta^{15}N^{bulk}$ and SP, respectively

Figure 2: Target gas (red) and surface layer (black) N_2O mole fractions (top) and δ-values (three bottom panels) measured in the atmospheric surface layer in 2.2 m height during the field campaign. Each couple of vertical dashed blue lines indicates the management events mowing (first line) and fertilization (second line).

Figure 3: Noon-to-noon averaged N_2O flux (f_{N2O}), overnight increase in N_2O mole fractions (difference in minimum and maximum N_2O concentration in a noon-to-noon period; δN_2O), Keeling-plot derived isotopic composition of soil-emitted N_2O (SP, $\delta^{15}N^{bulk}$, $\delta^{18}O$), nutrient concentrations (ammonium, nitrate and dissolved organic carbon; DOC), water filled pore space (wfps), precipitation (prcp) and soil temperature (T) over the measurement period. Each couple of vertical dashed blue lines indicates the management events mowing (first line) and fertilization (second line). Transparent blue boxes represent periods of N_2O emission influenced by management or rewetting (third box).

Figure 4: Standard error for SP (ε_{SP}) of soil-derived N_2O estimated by the Keeling plot approach as function of overnight N_2O accumulation in the surface layer. The red dashed lines show 12 ppb increase in N_2O mole fractions. Red full circles represent the selected subset.

Figure 5: SP - NH_4^+ / NO_3^- and SP - wfps / soil temperature maps. The size of the points is inversely scaled to Keeling plot intercept standard error so that biggest points are those with lowest uncertainty.

882 **Figure 6:** Boxplots for Keeling-plot derived SP, $\delta^{15}N^{bulk}$, $\delta^{18}O$ of soil-emitted N_2O and wfps of management events
883 (Mana I – III), rainfall after a dry period (Rewetting), and the remaining measurement period (BG).
884
885 **Figure 7:** Left panel: map of SP/$\delta^{15}N^{bulk}$ with rectangles representing process groups N_2O_N and N_2O_D based on SP
886 values in Decock and Six (2013b) and $\delta^{15}N^{bulk}$ estimated from minimum and maximum fractionation factors reported
887 in Baggs (2008) and substrate isotopic compositions reported by Bedard-Haughn et al (2003), Pörtl et al. (2007) and
888 Toyoda et al. (2011). Right panel: map of SP/$\delta^{18}O$ with traces of management events (ManaI in black, ManaII in red,
889 ManaIII in green) and the rewetting event (blue). Isotopic compositions are plotted for the transparent blue boxes in
890 Fig. 3 including one preceding and one following composition. The preceding composition is represented by the
891 enlarged filled triangle and transparency of the line connecting the compositions decreases with event duration.
892
893

Figures

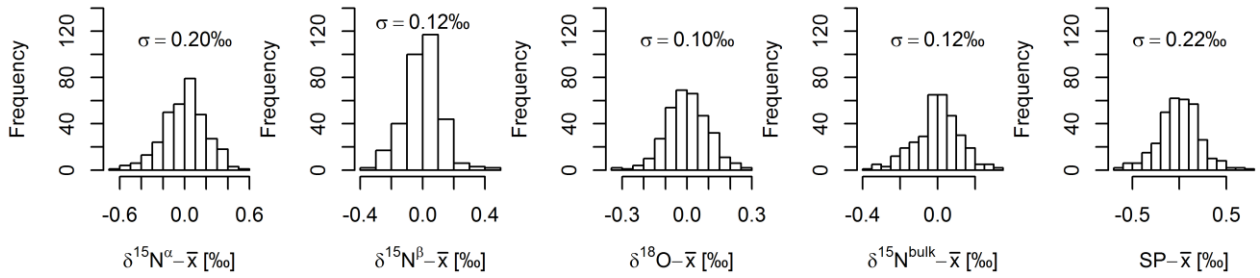

Figure 1

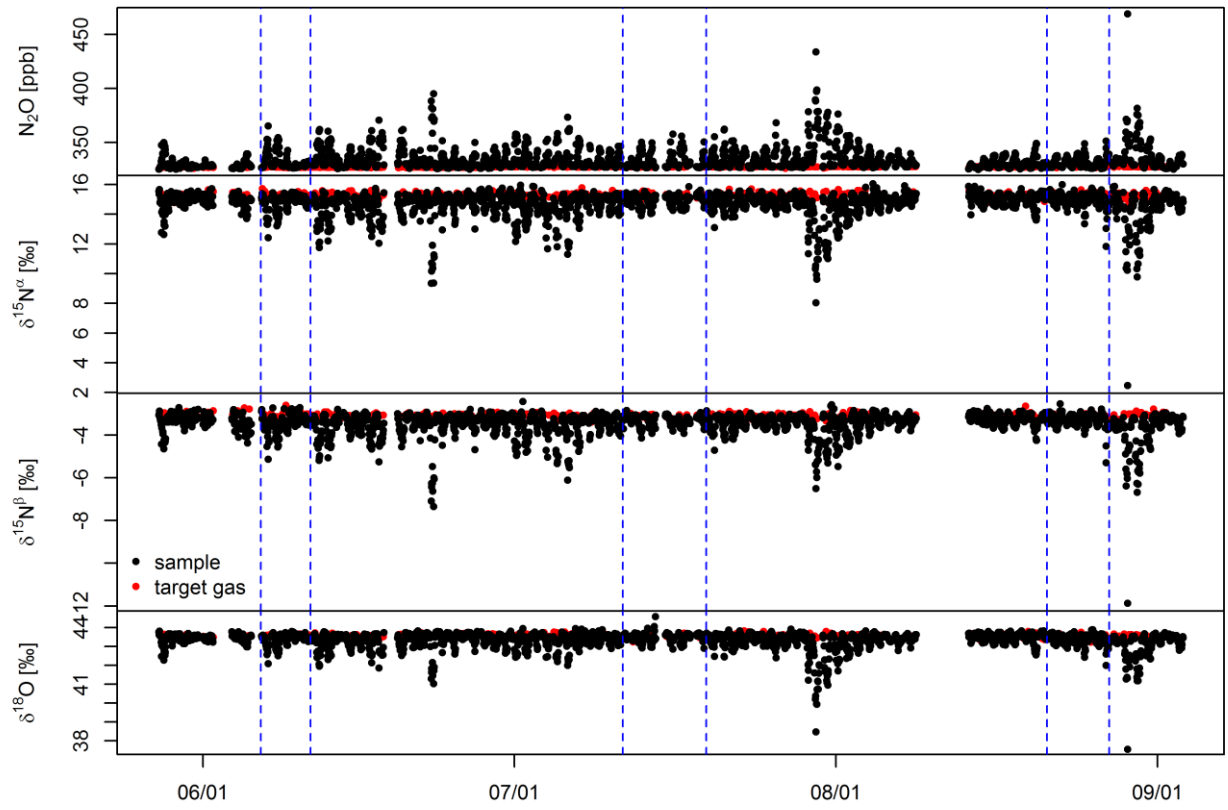

Figure 2

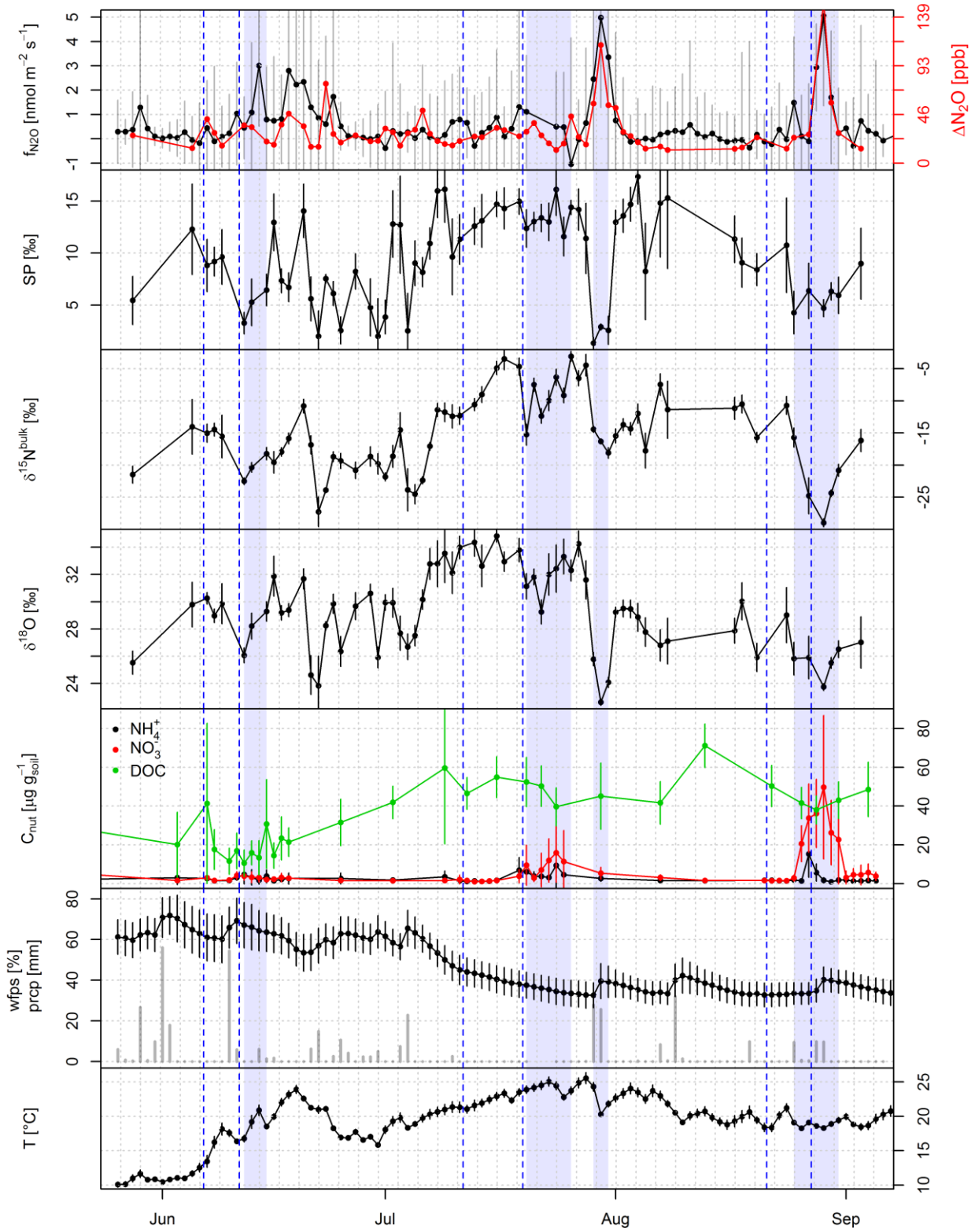

900

901 Figure 3

902

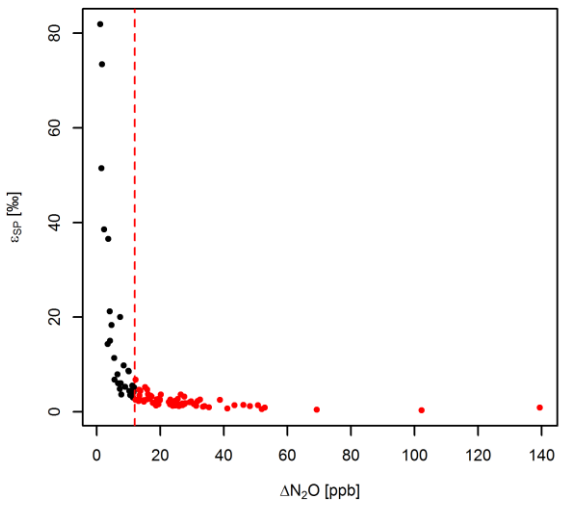

903

904 Figure 4

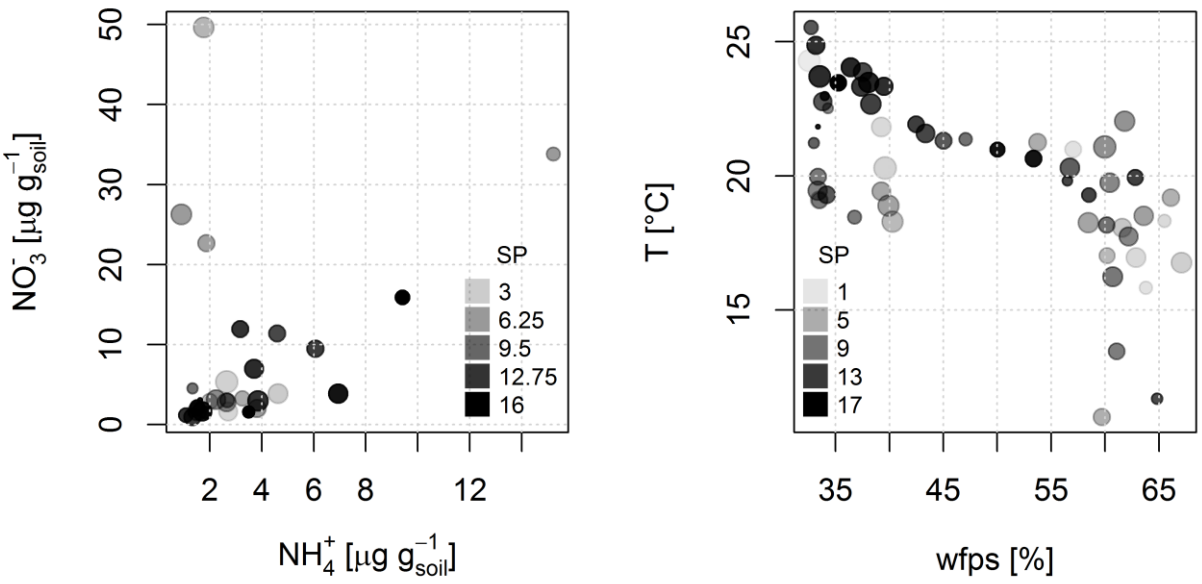

905

906 Figure 5

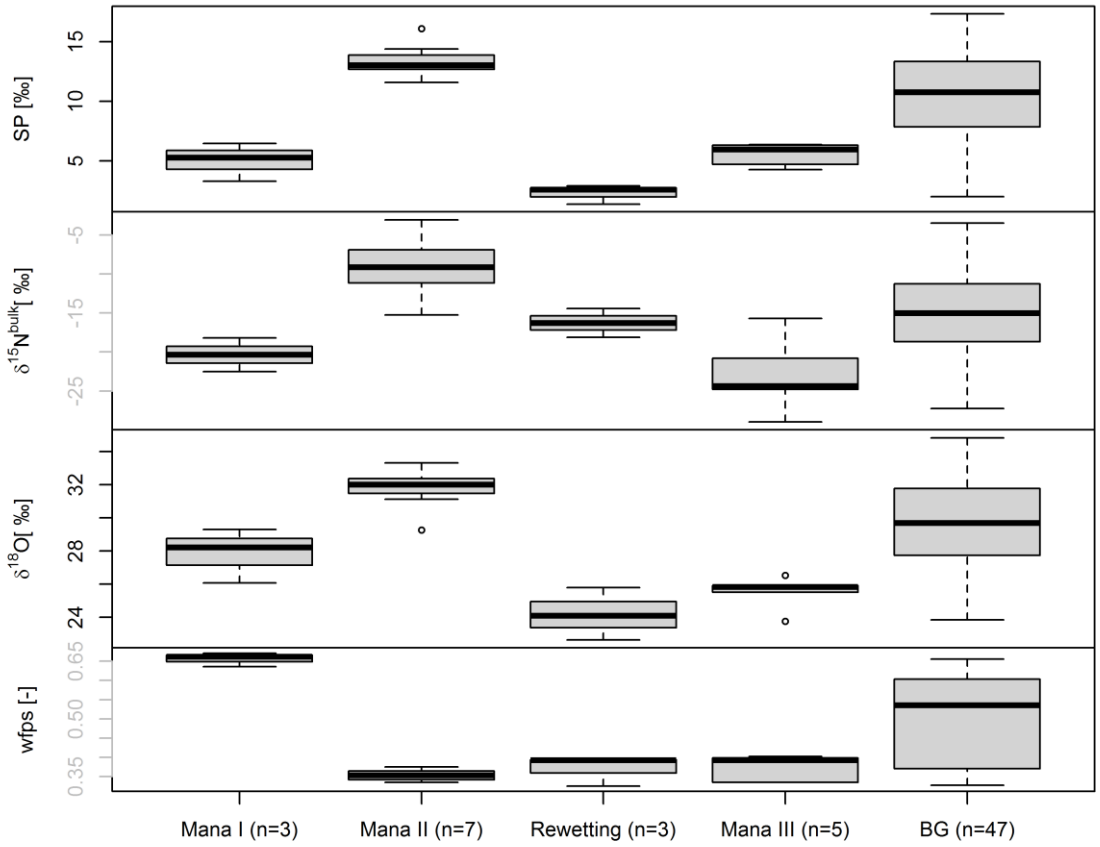

907

908 Figure 6

909

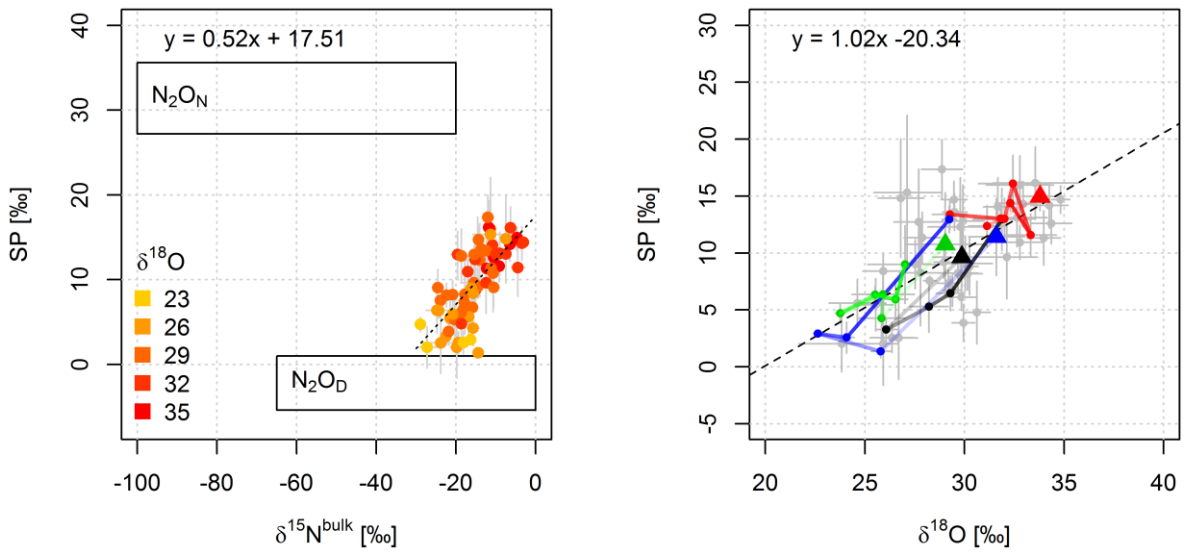

910

911 Figure 7